Theoretical Investigation on the Rotational Isomerism of Calix[4]arenes: Influence of the Hydroxyl → Methoxy Replacement

Carlos Alemán*,† and Jordi Casanovas*,‡

Departament d'Enginyeria Química, E. T. S. d'Enginyeria Industrial de Barcelona, Universitat Politècnica de Catalunya, Diagonal 647, Barcelona E-08028, Spain, and Departament de Química, Escola Politècnica Superior, Universitat de Lleida, c/Jaume II No. 69, Lleida E-25001, Spain

Received: June 23, 2005; In Final Form: July 15, 2005

The rotational isomerism of calix[4]arene, 25,27-dihydroxy-26,28-dimethoxycalix[4]arene, and 25,26,27,28-tetramethoxycalix[4]arene in different environments has been examined using sophisticated ab initio and DFT calculations. Free energies in the gas phase, in chloroform, and in toluene have been calculated not only for the minimum energy conformations cone and paco, which differ in the orientation of one phenol/anisole ring with respect to the other three, but also for the transition state that connects these two minima. Results provide a complete understanding of the changes induced by the partial or total OH → OCH_3 replacement in the calix[4]arene scaffold.

Introduction

Calixarenes, synthetic macrocyclic molecules built from phenolic units, are used as building blocks in supramolecular chemistry and selective ion binders. The simplest representation of these macrocycles is the calix[4]arene (**1**), which consists of

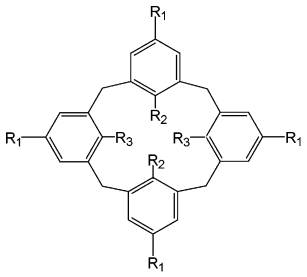

1: R_1= H, R_2= R_3= OH

2: R_1= ^{t}Bu, R_2= R_3= OH

3: R_1= H, R_2= OH, R_3= OCH_3

4: R_1= H, R_2= R_3= OCH_3

four phenol units connected via methylene bridges in the ortho positions with respect to the hydroxyl group. However, many other compounds have been prepared by introducing selective chemical modifications, the more common being at the phenolic hydroxy groups, the para position of the rings, and the methylene bridge.[1−3]

The methylene bridging groups, which allow the rotation of the phenolic rings, provide a notable conformational flexibility to **1** and its derivatives. Thus, the most relevant conformations are those denoted cone and partial-cone (paco), which differ in the orientation of one phenol ring with respect to the other three (Figure 1). The dynamic equilibrium between the cone and paco conformations have been studied in solution using NMR

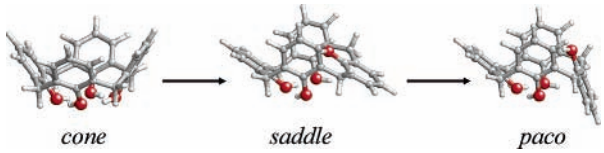

Figure 1. Characteristic conformations of calix[4]arene (**1**).

spectroscopy.[1,3] In the past decade, the cone-to-paco transition of **1** and selected simple derivatives has been investigated using theoretical methods. The aim of such studies was to understand and rationalize the conformational characteristics of these versatile molecules. Accordingly, the conformational inversion of **1** was studied in a vacuum, benzene, and chloroform by sophisticated molecular dynamics (MD) simulations.[4] More recently, the same authors reported the isomerization rate of *p-tert*-butylcalix[4]arene (**2**) in a vacuum and in chloroform.[5] The influence of the solvent on the conformational isomerism of **1** and **2** was also studied using the quantum mechanical and semiclassical formalisms of a widely used continuum model.[6] Furthermore, simple molecular mechanics calculations based on energy minimization and conventional MD were performed on derivatives of **1**.[3e,f,7,8] Ab initio calculations were also applied on related calixarenes to study the complexation and other aspects of these impartant compounds.

In this study, sophisticated quantum mechanical methods in a vacuum and in solution are used to examine the changes produced in the cone-to-paco conformational transition when phenolic hydroxyl groups of **1** are partially or totally replaced by methoxy groups. For this purpose, ab initio Hartree−Fock (HF) and density functional theory (DFT) calculations have been performed on **1** and two derivatives, i.e., 25,27-dihydroxy-26,-28-dimethoxycalix[4]arene (**3**) and 25,26,27,28-tetramethoxycalix-[4]arene (**4**). Results have been compared with available experimental data on related compounds.

Methods

All the calculations were performed at the "Centre de Supercomputació de Catalunya" (CESCA) and "Centre Europeu de Paral·lelisme de Barcelona" (CEPBA) using Gaussian 98.[9]

* Corresponding authors.
† Universitat Politècnica de Catalunya. E-mail: carlos.aleman@upc.es. Phone: 34-93401-0883.
‡ Universitat de Lleida. E-mail: jcasanovas@quimica.udl.es. Phone: 34-97370-2783.

10.1021/jp053404s CCC: $30.25
Published on Web 08/12/2005

Molecular Conformations. Three different conformational states were considered for each compound. These were the cone, the paco, and the saddle point conformations (Figure 1), the latter being the transition state of the cone-to-paco conformation. The cone and paco minimum energy conformations were derived from full geometry optimizations, whereas an appropriate constraint was applied to obtain the saddle conformation.

Gas-Phase Calculations. All the ab initio calculations were performed at the HF level, whereas two different functionals were employed for DFT calculations. More specifically, we used the following combinations: the Becke's three-parameter hybrid functional (B3) with the Lee, Yang, and Parr (LYP) expression for the nonlocal correlation (B3LYP);[10] and the same functional with the nonlocal correlation provided by Perdew and Wang's (B3PW91).[11] In both HF and DFT calculations, 6-31G(d), 6-311G(d,p), and 6-311++G(d,p) basis sets were used.[12,13] Frequency analyses were carried out to verify the minimum state or saddle point nature of all the stationary points located during HF/6-31G(d) and HF/6-311G(d,p) geometry optimizations. However, frequency calculations were not possible for the structures obtained using DFT methods, because they require a very huge amount of computational resources. The computed frequencies were used to obtain the zero-point vibrational energies (ZPVE) and both the thermal and entropic corrections. The conformational Gibbs free energies in the gas phase were obtained by adding such statistical corrections to the gas-phase electronic energies.

Solution Calculations. To obtain an estimation of the solvation effects, single point calculations were also conducted on the gas-phase optimized geometries using a self-consistent reaction-field (SCRF) model. SCRF methods treat the solute at the quantum mechanical level, and the solvent is represented as a dielectric continuum. Specifically, we chose the polarizable continuum model (PCM) developed by Tomasi and co-workers to describe the bulk solvent.[14] The PCM represents the polarization of the liquid by a charge density appearing on the surface of the cavity created in the solvent, i.e., the solute/solvent interface. This cavity is built using a molecular shape algorithm. It should be emphasized that the reliability of this method to describe the solvation effects on the conformational equilibrium of calix[4]arene was recently proved.[6]

PCM calculations were performed in the framework of the HF/6-31G(d) and B3LYP/6-31G(d) level using the standard protocol and considering the dielectric constant of chloroform ($\epsilon = 4.9$) and toluene ($\epsilon = 2.4$). The conformational free energies in solution (ΔG_{conf}) were estimated using the classical thermodynamical scheme: the free energies of solvation (ΔG_{sol}) provided by the PCM model were added to conformational Gibbs free energies in the gas phase.

Results and Discussion

Calix[4]arene (1). Table 1 lists the energies of the saddle and the paco conformations relative to the cone one (ΔE^{sadd} and ΔE^{paco}, respectively) calculated using different theoretical methods, which differ in the level used for geometry optimization and/or energy evaluation. Table 2 shows the relative free energies in the gas phase (ΔG_{gp}^{sadd} and ΔG_{gp}^{paco}) calculated using the HF/6-31G(d) and HF/6-311G(d,p) optimized geometries. These results allow us to discern the influence of the computational method and the size of the basis set on the conformational inversion studied in this work.

As can be seen, B3LYP and B3PW91 geometry optimizations led to similar values of ΔE^{sadd} and ΔE^{paco}, the differences between the two functionals being small for both the 6-31G(d) and 6311G(d,p) basis sets. Furthermore, within a given method the relative energies decrease with the size of the basis set independently of the level of geometry optimization. For instance, the values of ΔE^{paco} and ΔE^{sadd} obtained at the B3LYP/6-31G(d)//B3LYP/6-31G(d) level, where this notation refers to level of energy calculation//level of geometry optimization, are 2.4 and 2.1 kcal/mol, respectively, higher than the values derived from B3LYP/6-311++G(d,p)//B3LYP/6-31G(d) calculations. On the other hand, the overall results displayed in Table 1 clearly shows that the DFT relative energies are larger than the HF ones independently of the method used for geometry optimization. For example, HF/6-311++G(d,p)//HF/6-31G(d) and HF/6-311++G(d,p)//B3LYP/6-31G(d) relative energies differ by less than 0.2 kcal/mol, whereas comparison between the latter level and the B3LYP/6-311++G(d,p)//B3LYP/6-31G(d) one reveals differences of 2.5 kcal/mol. Considering the size of the molecules under study, the 6-311++G(d,p) basis set is expected to be sufficiently extended and flexible to calculate properly the electronic energy.

Comparison between the ΔG_{gp}^{sadd} and ΔG_{gp}^{paco} predicted at the HF/6-31G(d)//HF/6-31G(d) and HF/6-311G(d,p)//HF/6-311G(d,p) levels (Table 2) reveals an excellent agreement, the largest difference being 1.1 kcal/mol. Thus, reliable estimations of the ZPVE and statistical corrections are derived from HF/6-31G(d) geometries. Considering the results displayed in Tables 1 and 2, our best ab initio and DFT estimates of the free energies for the larger compounds will be obtained at the HF/6-311++G(d,p)//HF/6-31G(d) and B3LYP/6-311++G(d,p)//HF/6-31Gd) levels, respectively: the energies provided by the 6-311++G(d,p) basis set will be corrected by addition of the ZPVE and thermal and entropic contributions calculated using HF/6-31G(d) frequencies. Table 2 lists the ΔG_{gp}^{sadd} and ΔG_{gp}^{paco} values derived for **1** using such procedures, as well as those estimated

TABLE 1: Gas-Phase Energies (kcal/mol) of the Paco and Saddle Conformations Relative to the Cone Minimum of 1 Calculated Using Different Theoretical Methods

theoretical method[a]	ΔE^{paco}	ΔE^{sadd}
HF/6-31G(d)//HF/6-31G(d)	7.4	14.9
B3LYP/6-31G(d)//B3LYP/6-31G(d)	10.4	18.5
B3PW91/6-31G(d)//B3PW91/6-31G(d)	9.4	17.8
HF/6-311G(d,p)//HF/6-311G(d,p)	6.3	14.9
B3LYP/6-311G(d,p)//B3LYP/6-311G(d,p)	9.1	16.9
B3PW91/6-311G(d,p)//B3PW91/6-311G(d,p)	8.0	16.1
HF/6-311G(d,p)//HF/6-31G(d)	6.3	14.9
HF/6-311++G(d,p)//HF/6-31G(d)	5.3	14.0
B3LYP/6-311G(d,p)//HF/6-31G(d)	9.3	16.7
B3LYP/6-311++G(d,p)//HF/6-31G(d)	7.7	15.5
HF/6-311G(d,p)//B3LYP/6-31G(d)	6.1	14.3
HF/6-311++G(d,p)//B3LYP/6-31G(d)	5.5	13.9
B3LYP/6-311G(d,p)//B3LYP/6-31G(d)	9.2	17.1
B3LYP/6-311++G(d,p)//B3LYP/6-31G(d)	8.0	16.4

[a] Level of energy calculation//level of geometry optimization.

TABLE 2: Free Energies in the Gas Phase (kcal/mol) of the Paco and Saddle Conformations Relative to the Cone Minimum of 1 Predicted by Different Theoretical Methods

	ΔG_{gp}^{paco}	ΔG_{gp}^{sadd}
HF/6-31G(d)//HF/6-31G(d)[a]	5.8	13.6
HF/6-311G(d,p)//HF/6-311G(d,p)[a]	4.7	13.6
HF/6-311++G(d,p)//HF/6-31G(d)[a]	3.7	12.7
B3LYP/6-311++G(d,p)//HF/6-31G(d)[a]	6.1	14.2
den Otter et al.[b] (force-field)	7.9	13.1
Fischer et al.[c] (force-field)	8.9	

[a] Level of energy calculation//level of geometry optimization and frequency calculations. [b] Reference 4a. [c] Reference 7a.

TABLE 3: Free Energies of Solvation (kcal/mol) in Chloroform and Toluene Computed for the Cone, Paco, and Saddle Conformational States of 1 by Using Different Quantum Mechanical Frameworks of the PCM Model

solvent	method[a]	ΔG_{sol}^{cone}	ΔG_{sol}^{paco}	ΔG_{sol}^{sadd}
chloroform	HF/6-31G(d)	−0.6	3.7	2.9
	B3LYP/6-31G(d)	0.5	2.9	2.3
toluene	HF/6-31G(d)	2.2	4.4	3.4
	B3LYP/6-31G(d)	2.2	4.6	3.8

[a] Method used for PCM calculations in solution. The geometries obtained in the gas phase at the HF/6-31G(d) level were used in all cases.

by other authors using force-field calculations.[4a,7a] The latter agree very well with our quantum mechanical estimations.

Table 3 lists the free energies of solvation calculated for the cone, paco, and saddle conformations (ΔG_{sol}^{cone}, ΔG_{sol}^{paco}, and ΔG_{sol}^{sadd}) in chloroform and toluene. The PCM method was applied within the HF/6-31G(d) and B3LYP/6-31G(d) frameworks, the geometries optimized in the gas phase at the HF/6-31G(d) level being used for such calculations. Although the differences between the free energies of solvation predicted by the two methods decrease with the molecular size of the solvent, i.e., the largest difference is 0.4 and 1.1 kcal/mol in toluene and chloroform, respectively, the agreement is very good. In all cases the cone conformation presents the most favorable interaction with the solvent, and the worst solvation is for paco.

The conformational free energies in chloroform and toluene were computed by adding the free energies of solvation to the relative free energies in the gas phase. Table 4 compares the estimations for paco and saddle ($\Delta\Delta G_{conf}^{paco}$ and $\Delta\Delta G_{conf}^{sadd}$) relative to cone, which are based on the application of HF [gas phase at HF/6-311++G(d,p)//HF/6-31G(d) and PCM at HF/6-31G(d)] and B3LYP [gas phase at B3LYP/6-311++G(d,p)//HF/6-31G(d) and PCM at B3LYP/6-31G(d)] quantum mechanical methods, with experimental data[15] and molecular dynamics values.[4a]

As can be seen, NMR experiments indicate that $\Delta\Delta G_{conf}^{sadd}$ is 1.0 kcal/mol larger in chloroform than in toluene.[15] HF calculations reproduce qualitatively this difference (2.3 kcal/mol), whereas the B3LYP method underestimates it by 0.8 kcal/mol. Similarly, comparison of the $\Delta\Delta G_{conf}^{sadd}$ values indicates that the agreement with experimental data is very good for both HF and B3LYP values. Thus, the $\Delta\Delta G_{conf}^{sadd}$ in chloroform and toluene derived from HF calculations differ from the experimental values by less than 1.3 kcal/mol, whereas application of B3LYP calculations increases this threshold differences to 1.9 kcal/mol.

On the other hand, den Otter et al.[4a] investigated the isomerization rate of **1** in chloroform using classical molecular dynamics simulations. The $\Delta\Delta G_{conf}^{sadd}$ predicted by this force-field method was in very good agreement with the experimental value; i.e., they differ by only 1.3 kcal/mol, whereas $\Delta\Delta G_{conf}^{paco}$ is 1.1 and 0.6 kcal/mol larger than the HF and B3LYP estimations, respectively. Although no force-field simulation has been reported in toluene solution yet, den Otter et al.[4a] extended their study to benzene solution. The values calculated for $\Delta\Delta G_{conf}^{paco}$ and $\Delta\Delta G_{conf}^{sadd}$ in the latter solvent, which is similar to toluene, were 8.4 and 12.5 kcal/mol, respectively.

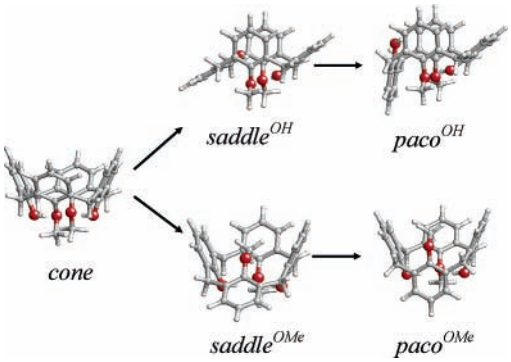

Figure 2. Characteristic conformations of 25,27-dihydroxy-26,28-dimethoxycalix[4]arene (**3**).

In summary, the overall of the results indicates that single point calculations at the HF/6-311++G(d,p) level on HF/6-31G(d) geometries provide reliable gas-phase energies, whereas good solvation free energies are derived from PCM calculations at the HF/6-31G(d) level. The excellent results provided by this computational scheme are probably due to a cancellation of errors. Despite this, such a computational procedure will be used in the next sections to study the cone-to-paco conformational transitions in **3** and **4**. However, to provide a deeper insight about the influence of electron correlation in these conformational transitions, single point calculations have been also performed in the gas phase at the B3LYP/6-311++G(d,p) level using the HF/6-31G(d) geometries.

25,27-Dihydroxy-26,28-dimethoxycalix[4]arene (3). For this compound two representative saddle and paco conformations can be distinguished depending on the rotated ring. We have denoted these states as saddle^{OH} and paco^{OH} when the rotation involves a phenol ring and as saddle^{OMe} and paco^{OMe} when the ring that changes the orientation with respect to the other three contains a methoxy group (i.e., the rotation involves an anisole ring). The five conformational states investigated for **3** are displayed in Figure 2. Table 5 shows the relative free energies in the gas phase, and the conformational free energy differences in chloroform and toluene are listed in Table 6.

The replacement of two hydroxyl groups by two methoxy groups produces the loss of two O−H···O hydrogen bonds. Consequently, the distances between the oxygen atoms belonging to adjacent rings are expected to increase with respect to **1**. Thus, the four O···O distances predicted for the cone conformation of **3** are 2.808, 3.003, 2.808, and 3.003 Å, in good agreement with those reported for its X-ray molecular structure[16]

TABLE 4: Conformational Free Energies (kcal/mol) in Chloroform and Toluene Solution of the Paco and Saddle Conformations Relative to the Cone Minimum of 1 Provided by Different Theoretical Methods

solvent	method[a]	$\Delta\Delta G_{conf}^{paco}$	$\Delta\Delta G_{conf}^{sadd}$
chloroform	HF/6-311++G(d,p)//HF/6-31G(d) [PCM-HF/6-31G(d)]	8.0	16.2
	B3LYP/6-311++G(d,p)//HF/6-31G(d) [PCM-B3LYP/6-31G(d)]	8.5	16.0
	den Otter et al.[b] (force-field)	9.1	13.6
	exp[c] (NMR)		14.9
toluene	HF/6-311++G(d,p)//HF/6-31G(d) [PCM-HF/6-31G(d)]	5.9	13.9
	B3LYP/6-311++G(d,p)//HF/6-31G(d) [PCM-B3LYP/6-31G(d)]	8.5	15.8
	exp[c] (NMR)		13.9

Experimental values obtained using NMR are included. [a] Method: gas-phase calculation [solution calculation]. [b] Reference 4a. [c] Reference 15.

TABLE 5: Free Energies in the Gas Phase (kcal/mol) of the Paco^{OH}, Paco^{OMe}, Saddle^{OH}, and Saddle^{OMe} Conformations Relative to the Cone Minimum of 3 Predicted by Different Theoretical Methods

	$\Delta G_{gp}^{paco-OH}$	$\Delta G_{gp}^{paco-OMe}$	$\Delta G_{gp}^{sadd-OH}$	$\Delta G_{gp}^{sadd-OMe}$
HF/6-31G(d)//HF/6-31G(d)[a]	1.7	6.5	9.2	29.1
HF/6-311++G(d,p)//HF/6-31G(d)[a]	0.7	6.5	8.7	28.6
B3LYP/6-311++G(d,p)//HF/6-31G(d)[a]	0.7	5.7	7.8	23.4
Grootenhuis et al.[b] (force-field)	0.1			

[a] Level of energy calculation//level of geometry optimization and frequency calculations. [b]Reference 7b.

TABLE 6: Conformational Free Energies (kcal/mol) in Chloroform and Toluene Solution[a] of the Paco^{OH}, Paco^{OMe}, Saddle^{OH}, and Saddle^{OMe} Conformations Relative to the Cone Minimum of 3

solvent	$\Delta\Delta G_{conf}^{paco-OH}$	$\Delta\Delta G_{conf}^{paco-OMe}$	$\Delta\Delta G_{conf}^{sadd-OH}$	$\Delta\Delta G_{conf}^{sadd-OMe}$
chloroform	0.6	5.5	7.7	26.7
toluene	0.9	6.4	8.7	26.7

[a] Gas-phase and PCM calculations at the HF/6-311++G(d,p)//HF/6-31G(d) and HF/6-31G(d) levels, respectively.

(2.86, 2.93, 2.92 and 2.96 Å), whereas those calculated for the cone conformation of **1** at the same level of theory are equal to 2.739 Å.

Inspection to the free energies in the gas phase (Table 5) indicates that the values obtained at the HF/6-311++G(d,p)//HF/6-31G(d) and B3LYP/6-311++G(d,p)//HF/6-31G(d) levels are fully consistent. The cone conformation with the methoxy groups pointing outward is the most stable conformation in the gas phase, although paco^{OH} is only 0.7 kcal/mol less favored. Thus, the change from cone-to-paco^{OH} produces the loss of another O−H···O hydrogen bonds, although this is partially compensated for by a reduction in the electrostatic repulsion between the oxygen atoms. Furthermore, it should be noted that the extra-energy gain produced by the formation of four consecutive hydrogen bonds in the cone conformation of **1**, i.e., hydrogen bonding cooperative effects,[17] is absent in **3**, leading to a reduction in the stability of its cone conformation. Grootenhuis et al.[7b] used molecular mechanics calculations to predict that cone and paco^{OH} are conformations of comparable energy; i.e., a difference of 0.1 kcal/mol was obtained, in agreement with the present calculations.

On the other hand, the free energy in the gas phase of the paco^{OMe} conformation is around 6 kcal/mol, indicating that this arrangement is considerably less stable than paco^{OH}. Interestingly, the paco^{OMe} conformation contains two O−H···O hydrogen bonds as the cone arrangement. This is because the oxygen atom of the methoxy group acts as a hydrogen bond acceptor of the two hydroxyl groups that act as donors; i.e., one of the two hydroxyl groups changes the orientation during minimization (Figure 2). However, the repulsive steric interactions produced by the methyl group of the rotated ring in the cavity of the calix[4]arene are not compensated by this second hydrogen bond, explaining the low stability of paco^{OMe} with respect to paco^{OH}.

The conformational free energies in the gas phase of the saddle^{OH} transition state with respect to the cone conformation range from 7.8 to 9.2 kcal/mol depending on the computational method. These values are 4.4−6.4 kcal/mol smaller than those predicted for the saddle of **1** using the same methods. This difference is probably due to the stability of the cone conformation that, as discussed above, is higher for **1** than for **3**. Consequently, the isomerization barrier is lower for the latter compound. On the other hand, the saddle^{OMe} barrier is very unfavored with respect to saddle^{OH}, the values of $\Delta G_{gp}^{sadd-OMe}$ predicted at the HF/6-311++G(d,p) and B3LYP/6-311++G(d,p) levels being 23.4 and 28.6 kcal/mol, respectively. These

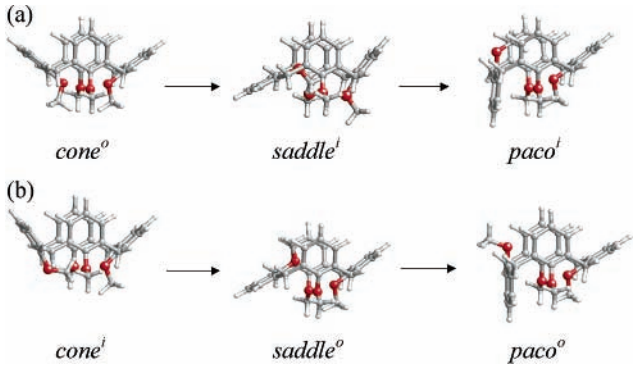

Figure 3. Characteristic conformations of 25,26,27,28-tetramethoxycalix[4]arene (**4**).

results indicate that the inward orientation of the methyl group contained in the rotated anisole ring, i.e., filling the calix[4]arene cavity (Figure 2), produces strong repulsive interactions.

Results displayed in Table 6 indicate that the role of the solvent on the conformational isomerism of **3** is very small. Thus, the free energy differences in solution, especially in toluene, are similar to those obtained in the gas phase. Regarding to the results, the largest difference was obtained for saddle^{OMe}, which is 1.9 kcal/mol more stable with respect to cone in both chloroform and toluene solution than in the gas phase.

25,26,27,28-Tetramethoxycalix[4]arene (4). The lowest cone conformation corresponds to that in which all the methoxy groups point outward (cone°). To minimize the repulsive interactions between the methoxy groups, the anisole rings are slightly rotated with respect to the phenol rings of **1** (Figure 3a). The O···O distances predicted for the cone° conformation of **4** are 3.195, 3.187, 3.195, and 3.187 Å, these values being about 0.45 Å larger than those computed for **1**. The rotation of one anisole unit, using as starting point the favored cone° arrangement, produces a paco conformation with the methoxy group pointing inward, which has been denoted paco^{i}. The rotational isomerism processes cone° → paco^{i} is displayed in Figure 3a and the free energies in the gas phase are listed in Table 7. The free energy in the gas phase of paco^{i} is less favored than that of cone° by 8.4 and 6.8 kcal/mol at the HF/6-311++G(d,p)//HF/6-31G(d) and B3LYP/6-311++G(d,p)//HF/6-31G(d) levels, respectively. Saddle^{i}, which connects cone° with paco^{i}, is unfavored by 33.0 and 27.1 kcal/mol at the same levels of theory. This energy barrier, which indicates that the cone° → paco^{i} rotational isomerism is energetically forbidden, is even ∼4 kcal/mol higher than that calculated for **3**.

The effect of the chloroform and toluene solvents on the cone° → paco^{i} process is showed in Table 8, which lists the conformational free energy differences in solution. As can be seen, the organic solvents tend to stabilize both the saddle^{i} and paco^{i} states by about 3 kcal/mol. In an early study, Iwamoto et al.[3g] investigated the conformer distribution of **4** in $CDCl_3$ using NMR. The authors found that the population of paco is higher than that of cone by more than 2 times, indicating that the latter conformation is less stable than the former, i.e., about 0.6 kcal/

TABLE 7: Free Energies in the Gas Phase (kcal/mol) of the Cone^i, Paco^i, Paco°, Saddle^i, and Saddle° Conformations Relative to the Cone° Minimum of 4 Predicted by Different Theoretical Methods

	$\Delta G_{gp}^{cone,i}$	$\Delta G_{gp}^{paco,i}$	$\Delta G_{gp}^{paco,\circ}$	$\Delta G_{gp}^{sadd,i}$	$\Delta G_{gp}^{sadd,\circ}$
HF/6-31G(d)//HF/6-31G(d)[a]	12.5	7.2	1.1	33.3	15.3
HF/6-311++G(d,p)//HF/6-31G(d)[a]	13.6	8.4	1.5	33.0	15.4
B3LYP/6-311++G(d,p)//HF/6-31G(d)[a]	10.2	6.8	1.6	27.1	13.3
Iwamoto et al.[b] (force-field)			−0.3		

[a] Level of energy calculation//level of geometry optimization and frequency calculations. [b] Reference 3g.

TABLE 8: Conformational Free Energies (kcal/mol) in Chloroform and Toluene Solution[a] of the Cone^i, Paco^i, Paco°, Saddle^i, and Saddle° Conformations Relative to the Cone° Minimum of 4[b]

solvent	$\Delta\Delta G_{conf}^{cone,i}$	$i\Delta\Delta G_{conf}^{paco,i}$	$\Delta\Delta G_{conf}^{paco,\circ}$	$\Delta\Delta G_{conf}^{sadd,i}$	$\Delta\Delta G_{conf}^{sadd,\circ}$
chloroform	16.3	5.5	2.0	29.4	12.6
toluene	16.8	5.7	1.6	29.3	12.8
Iwamoto et al.[c,d]			−0.6[c]		

[a] Gas-phase and PCM calculations at the HF/6-311++G(d,p)//HF/6-31G(d) and HF/6-31G(d), respectively. [b] Experimental values obtained using NMR are included. [c] Reference 3g. [d] NMR measurements in $CDCl_3$ solution.

mol.[3g] Furthermore, paco was also identified by NMR and X-ray crystallography as the preferred conformation of para-substituted analogues of **4**.[1b] These experimental results are in contradiction with the calculations presented in this study for the cone° → paco^i rotational isomerism.

To explain the disagreement between the present quantum mechanical calculations and the reported experimental data, the rotational isomerism of **4** was reinvestigated using as the starting point the cone conformation with one methyl group pointing inward (cone^i). This conformation, which is displayed in Figure 3b, is less favored than cone° by about 10−14 kcal/mol depending on the quantum mechanical method (Table 7). The rotation of the anisole unit with the methyl group pointing inward results in paco°. Figure 3b shows the rotational isomerism process cone^i → paco°, and Tables 7 and 8 include the calculated free energies in the gas phase and solution.

It is worth noting that paco° is about 5−7 kcal/mol more stable than paco^i in the gas phase. This fact is due to the steric repulsions, which are considerably weaker in the former. Moreover, the free energy in the gas phase of paco° is higher than that of cone° by only ∼1.5 kcal/mol. Force-field calculations reported by Iwamoto et al.[3g] predicted that paco° is 0.3 kcal/mol more stable than cone°. Furthermore, the free energy calculated in the gas phase for saddle° at the HF/6-311++G(d,p)//HF/6-31G(d) and B3LYP/6-311++G(d,p)//HF/6-31G(d) levels is 17.6 and 13.8 kcal/mol, respectively, lower than obtained for the saddle^i barrier. Indeed the saddle° barrier predicted for **4** is similar to that calculated for **1** using the same quantum mechanical procedures.

Calculations in chloroform and toluene solutions predict that paco° is less favored than cone° by 2.0 and 1.6 kcal/mol, respectively. Thus, the stability of the former conformation in chloroform solution is underestimated by 2.6 kcal/mol with respect to the experimental measurements of Iwamoto et al.[3g] This small difference is probably due to the limitations of the continuun solvation model employed in this study, i.e., omission of the interactions with the solvent molecules located in the first solvation shell, a poor description of the cavity formed by the phenol and/or anisole rings, etc. Indeed, it is known that the cone−paco equilibrium distribution of many calix[4]arenes is altered by the formation of host−guest complexes with solvent molecules.[1b,5,18] Molecular dynamics simulations in chloroform and benzene solutions showed that **1** is able to capture a solvent molecule from the bulk, even although this molecule is exchanged regularly.[4a] In comparison with **1**, the tendency of **4** to capture a solvent molecule is expected to be higher because, as can be deduced from the O···O distances, the central cavity of the latter is bigger. Unfortunately, the PCM method neglects the formation of such type of solute−solvent complexes, which could alter the influence of solvation on the conformational equilibrium of **4**.

On the other hand, the barrier saddle° is lower that saddle^i by more than a half. The overall of the results displayed in Tables 7 and 8 suggests that the complete rotational isomerism for **4** is cone° → cone^i → paco°. The last two states are separated by saddle°, whereas the transformation cone° → cone^i only involves the rotation of the single bond that connects the ring with the methoxy moiety. This path is in good agreement with the experimental data reported by Iwamoto et al.[3g]

Conclusions

The replacement of two opposite hydroxyl groups of **1** by methoxy groups produces a partial disruption of the cyclic array of intramolecular O−H···O hydrogen bonds associated with the cone conformation. Consequently, the stability of the paco conformations relative to the cone minimum decreases. Thus, the free energy of the paco^{OH} conformation with respect to the cone one is about 3−6 kcal/mol smaller, depending on the computational procedure and the environment, for **3** than for **1**. Furthermore, the energy barrier that separates the cone conformation from the paco^{OH} one is smaller for **3** than for **1** by about 1−6 kcal/mol, depending on the method and the environment. Therefore, our calculations predict that the equilibrium between the cone and its inverted paco^{OH} conformation is more dynamical for **3** than for **1**.

The total replacement of hydroxyl by methoxy groups, as occurs in **4**, enhances the relative stability of the paco conformation with respect to the cone one. Thus, as a consequence of the complete absence of O−H···O interactions, the latter conformation becomes even less favored in **4** than in **3**. Interestingly, the rotational isomerism cone°-to-paco° previously requires that the methyl group belonging to the rotated ring changes from an inward arrangement to an outward one. Accordingly, the complete conformational transition could be described as cone° → cone^i → paco°.

Acknowledgment. We are indebted to the CESCA and CEPBA for computational facilities and for generous allocation of computer time. This work was supported by MCYT and FEDER funds with Grant No. MAT2003-00251.

References and Notes

(1) (a) Biali, S. E.; Böhmer, V.; Cohen, S.; Ferguson, G.; Grüttner, C.; Grynszpan, F.; Paulus, E. F.; Thondorf, I.; Vogt, W. *J. Am. Chem. Soc.*

1996, *118*, 12938. (b) Soi, A.; Bauer, W.; Mauser, H.; Moll, C.; Hampel, F.; Hirsch, A. *J. Chem. Soc., Perkin Trans. 2* **1998**, 1471. (c) Gutsche, C. D. *Calixarenes*: The Royal Society of Chemistry, Cambridge, U.K., 1989.

(2) (a) León, S.; Leigh, D. A.; Zerbetto, F. *Chem. Eur J.* **2002**, *8*, 4854. (b) Parzuchowski, P.; Bohmer, V.; Biali, S. E.; Thondorf, I. *Tetrahedron-Asymmetry* **2000**, *11*, 2393.

(3) (a) Cajan, M.; Lhotak, P.; Lang, J.; Dvorakova, H.; Stibor, I.; Koca, J. *J. Chem. Soc., Perkin Trans. 2* **2002**, *11*, 1922. (b) Soi, A.; Bauer, A.; Mauser, H.; Moll, C.; Hampel, F.; Hirsch, A. *J. Chem. Soc., Perkin Trans. 2* **1998**, 1471. (c) Wöhnert, J.; Brenn, J.; Stoldt, M.; Alesiuk, O.; Grynszpan, F.; Thondorf, I.; Biali, S. E. *J. Org. Chem.* **1998**, *63*, 3866. (d) Biali, S. E.; Böhmer, V.; Brenn, J.; Frings, M.; Thondorf, I.; Vogt, W.; Wöhnert, J. *J. Org. Chem.* **1997**, *62*, 8350. (e) Van Gelder, J. M.; Brenn, J.; Thondorf, I.; Biali, S. E. *J. Org. Chem.* **1997**, *62*, 3511. (f) van Hoorn, W. P.; Briels, W. J.; van Duynhoven, J. P. M.; van Veggel, F. C. J. M.; Reinhoudt, D. N. *J. Org. Chem.* **1998**, *63*, 1299. (g) Iwamoto, K.; Ikeda, A.; Araki, K.; Harada, T.; Shinkai, S. *Tetrahedron* **1993**, *49*, 9937. (h) Ikeda, A.; Shinkai, S. *Chem. Rev.* **1997**, *97*, 1713.

(4) (a) den Otter, W. K.; Briels, W. J. *J. Am. Chem. Soc.* **1998**, *120*, 13167. (b) den Otter, W. K.; Briels, W. J. *J. Chem. Phys.* **1997**, *107*, 4968.

(5) Tolpekina, T. V.; Otter, W. K.; Briels, W. J. *J. Phys. Chem. B* **2003**, *107*, 14476.

(6) Alemán, C.; Otter, W. K.; Topekina, T. V.; Briels, W. J. *J. Org. Chem.* **2004**, *69*, 951.

(7) (a) Fischer, S.; Grootenhuis, P. D. J.; Groenen, L. C.; van Hoorn, W. P.; van Veggel, F. C. J. M.; Reinhoudt, D. N.; Karplus, M. *J. Am. Chem. Soc.* **1995**, *117*, 1611. (b) Grootenhuis, P. D. J.; Kollman, P. A.; Groenen, L. C.; Reinhoudt, D. N.; van Hummel, G. J.; Ugozzoli, F.; Andreetti, G. D. *J. Am. Chem. Soc.* **1990**, *112*, 4165. (c) Lipkowitz, K.; Pearl, G. *J. Org. Chem.* **1993**, *58*, 6729.

(8) (a) Choe, J. I.; Lee, S. H.; Oh, D. S. *Bull. Kor. Chem. Soc.* **2004**, *25*, 55. (b) Shatz, J. *Collect. Czech. Chem. Commun.* **2004**, *69*, 1169. (c) Novikov, A. N.; Bacherikov, V. A.; Gren, A. I. *Russ. J. Gen. Chem.* **2002**, *72*, 1396. (d) Billes, F.; Mohamed-Ziegler, I. *Supramol. Chem.* **2002**, *14*, 451. (e) Hay, B. P.; Nicholas, J. B.; Feller, D. *J. Am. Chem. Soc.* **2000**, *122*, 10083.

(9) Frisch, M. J.; Trucks, G. W.; Schlegel, H. B.; Scuseria, G. E.; Robb, M. A.; Cheeseman, J. R.; Zakrzewski, V. G.; Montgomery, Jr.; Stratmann, R. E.; Burant, J. C.; Dapprich, S.; Millam, J. M.; Daniels, A. D.; Kudin, K. N.; Strain, M. C.; Farkas, O.; Tomasi, J.; Barone, V.; Cossi, M.; Cammi, R.; Mennucci, B.; Pomelli, C.; Adamo, C.; Clifford, S.; Ochterski, J.; Petersson, G. A.; Ayala, P. Y.; Cui, Q.; Morokuma, K.; Malick, D. K.; Rabuck, A. D.; Raghavachari, K.; Foresman, J. B.; Cioslowski, J.; Ortiz, J. V.; Baboul, A. G.; Stefanov, B. B.; Liu, G.; Liashenko, A.; Piskorz, P.; Komaromi, I.; Gomperts, R.; Martin, R. L.; Fox, D. J.; Keith, T.; Al-Laham, M. A.; Peng, C. Y.; Nanayakkara, A.; Gonzalez, C.; Challacombe, M.; Gill, P. M. W.; Johnson, B.; Chen, W.; Wong, M. W.; Andres, J. L.; Gonzalez, C.; Head-Gordon, M.; Replogle, E. S.; Pople, J. A. *Gaussian 98*, revision A.7; Gaussian, Inc.: Pittsburgh, PA, 1998.

(10) (a) Becke, A. D. *J. Chem. Phys.* **1993**, *98*, 1372. (b) Lee, C.; Yang, W.; Parr, R. G. *Phys. Rev. B* **1993**, *37*, 785.

(11) Perdew, J. P.; Wang, Y. *Phys. Rev.* **1992**, *45*, 13244.

(12) Hariharan, P. C.; Pople, J. A. *Chem. Phys. Lett.* **1972**, *16*, 217.

(13) Frich, M. J.; Pople, J. A.; Krishnam, R.; Binkley, J. S. *J. Chem. Phys.* **1984**, *80*, 3264.

(14) (a) Miertus, M.; Scrocco, E.; Tomasi, J. *Chem. Phys.* **1981**, *55*, 117−129. (b) Miertus, S.; Tomasi, J. *Chem. Phys.* **1982**, *65*, 239−252.

(15) Gutsche, C. D.; Bauer, L. J. *J. Am. Chem. Soc.* **1985**, *107*, 6052.

(16) van Loon, J. D.; Arduini, A.; Verboom, W.; van Hummel, G. J.; Harkema, S.; Húngaro, R.; Reinhoudt, D. N. *Tetrahedron Lett.* **1989**, *30*, 2681.

(17) (a) Vicente, C.; Martin, J.; Jiménez-Barbero, J.; Chiara, J. L.; Vicent, C. *Chem. Eur. J.* **2004**, *10*, 4240. (b) Lin, J. Q.; Luo, S. W.; Wu, Y. D. *J. Comput. Chem.* **2002**, *23*, 1551. (c) Sum, A. K.; Sandler, S. I. *J. Phys. Chem. A* **2000**, *104*, 1121.

(18) Benevelli, F.; Bond, A.; Duer, M.; Klinowski, J. *Phys. Chem. Chem. Phys.* **2000**, *2*, 3977.